

Simultaneous assessment of rodent behavior and neurochemistry using a miniature positron emission tomograph

Daniela Schulz¹, Sudeepti Southekal^{2,5}, Sachin S Junnarkar³, Jean-François Pratte^{3,5}, Martin L Purschke⁴, Sean P Stoll⁴, Bosky Ravindranath², Sri Harsha Maramraju², Srilalan Krishnamoorthy², Fritz A Henn^{1,5}, Paul O'Connor³, Craig L Woody⁴, David J Schlyer^{1,2} & Paul Vaska^{1,2}

Positron emission tomography (PET) neuroimaging and behavioral assays in rodents are widely used in neuroscience. PET gives insights into the molecular processes of neuronal communication, and behavioral methods analyze the actions that are associated with such processes. These methods have not been directly integrated, because PET studies in animals have until now required general anesthesia to immobilize the subject, which precludes behavioral studies. We present a method for imaging awake, behaving rats with PET that allows the simultaneous study of behavior. Key components include the 'rat conscious animal PET' or RatCAP, a miniature portable PET scanner that is mounted on the rat's head, a mobility system that allows considerable freedom of movement, radiotracer administration techniques and methods for quantifying behavior and correlating the two data sets. The simultaneity of the PET and behavioral data provides a multidimensional tool for studying the functions of different brain regions and their molecular constituents.

In vivo neuroscience methods are indispensable for studies of brain function, especially when they can capture brain and behavioral processes in real time. Owing to the transient nature of these processes, information may be lost or altered when the brain is analyzed after the behavior took place. Electrophysiology can be used to monitor neuronal impulse activity during a behavioral task¹, fast-scan cyclic voltammetry and microdialysis measure local changes in neurotransmitter release^{2,3} in behaving animals and optical imaging techniques can assess calcium transients in mobile mice⁴. However, these methods are invasive and limited in the number of brain regions that can be assessed.

Noninvasive imaging of the whole brain in behaving animals, particularly in rodents, is highly desirable but has remained elusive. Typically, whole-brain imaging in animals requires general anesthesia to prevent motion artifacts, which precludes the

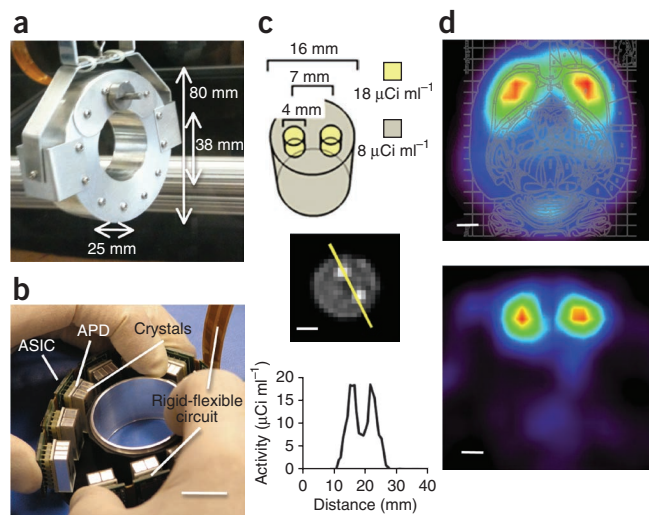
study of behavior and might disrupt neurochemistry^{5,6}. Some progress has been made with restraint devices and animal training, which allow whole-brain imaging in conscious but immobilized animals. Positron emission tomography (PET) is used in restrained animals to image metabolism, receptor occupancy and the activity of transporters and enzymes in the conscious brain^{5,7-9}. Functional magnetic resonance imaging can provide measures of metabolic activity during sensory stimulation, such as the presentation of odors and suckling pups¹⁰. Motion tracking of rodents that are allowed to move freely inside a PET scanner is under development¹¹, but the technical challenges are substantial and no quantitative brain imaging has been carried out under these conditions.

Our approach was to eliminate the restraint that is required for functional neuroimaging in the rat and thereby make it possible to directly correlate imaging data with simultaneously acquired behavioral data. The tools and methods we developed include a miniature high-performance PET scanner (RatCAP), which the rat wears on its head, mechanical methods for attaching the scanner and facilitating rat mobility, appropriate radiotracer strategies and ways to integrate PET data with behavioral measures.

Despite its diminutive size, the RatCAP had good spatial resolution and sufficient coincidence sensitivity for PET studies in the awake, behaving rat. The passive mechanical support system effectively compensated for the mass of the imager and facilitated rat motion with only temporary increases in stress hormone levels. We present PET results that indicate a correlation between dopamine D₂ receptor binding and spontaneous open field behavior, which might be related to autoreceptor function and tonic variations in dopamine¹². Dopamine has been implicated in several key functions such as motor control, the processing of reward and the formation and modulation of memories^{1,13-15}. The simultaneous study of PET and behavior is

¹Medical Department, Brookhaven National Laboratory, Upton, New York, USA. ²Department of Biomedical Engineering, Stony Brook University, Stony Brook, New York, USA. ³Instrumentation Division, Brookhaven National Laboratory, Upton, New York, USA. ⁴Physics Department, Brookhaven National Laboratory, Upton, New York, USA. ⁵Present addresses: Brigham & Women's Hospital, Boston, Massachusetts, USA (S.S.); Université de Sherbrooke, Sherbrooke, Quebec, Canada (J.-F.P.); Cold Spring Harbor Laboratory, Cold Spring Harbor, New York, USA (E.A.H.). Correspondence should be addressed to P.V. (vaska@bnl.gov).

Figure 1 | RatCAP tomograph and validation. **(a)** Assembled scanner with dimensions of enclosure. **(b)** Internal components during assembly, including lutetium yttrium oxyorthosilicate crystal arrays, avalanche photodiode arrays (APD), integrated circuit microchips (ASIC; not visible), and rigid-flexible printed circuit board. Scale bar, 2 cm. **(c)** Phantom validation study including the dimensions of the three-compartment phantom used in the study and the calibrated activity levels of [^{18}F]fluorodeoxyglucose in each compartment (top), a reconstructed image of the phantom (middle) and a profile through compartments with high radioactivity concentration (bottom). Scale bar, 5 mm. **(d)** PET images through striata of a conscious rat after a 0.75-mCi injection of [^{11}C]raclopride (5.4 nmol kg $^{-1}$ body weight), including a horizontal slice summed over the whole 1-h scan overlaid to scale with a rat brain atlas figure³⁰ without any adjustment for rat strain, sex or weight (top) and coronal slice from a single dynamic time frame spanning 35–45 min after injection (bottom). Scale bars, 2 mm.



not limited to investigations of the dopamine system and could be applied to various neurotransmitter systems using appropriate radiotracers and behavioral paradigms. PET in the awake, behaving animal should therefore be of interest to a broad range of neuroscientists.

RESULTS

RatCAP scanner

The RatCAP scanner is a small, complete-ring, fully functional PET system, weighing only 250 g, with an inner diameter of 38 mm, outer diameter of 80 mm and axial extent of 25 mm (Fig. 1a). It is positioned between the eyes and ears of the rat, allowing a normal forward-facing posture while imaging the whole brain with a field of view of 38-mm diameter by 18 mm axially. The spatial resolution is <2 mm full width at half maximum (FWHM) across the field of view and coincidence sensitivity is 0.76% at the center (Online Methods). Although in principle any brain region can be imaged, PET systems in general are limited in their ability to distinguish regions at the scale of the spatial resolution and below, and by the variation of the signal-to-noise ratio across the field of view (which is maximal in the center).

The development of the RatCAP involved several steps, including simulations of its feasibility¹⁶ and the development of specific components^{17–19}. To build a PET system sufficiently small to allow rats to move, we required compact and lightweight gamma-ray detectors and front-end readout electronics, as well as minimal external cabling. We chose the scintillator lutetium yttrium oxyorthosilicate (LYSO), which has among the highest detection efficiencies for PET, and thin, solid-state photosensors called avalanche photodiodes (Hamamatsu, S8550 APD), both in a 4 × 8 array geometry with a 2.2-mm square cross-section forming a detector block. A key development was a front-end microchip that conditions the 32 analog signals of the block, picks off the event time and serializes the data from the block into a single digital data output line¹⁷. Owing to the 1:1 coupling of scintillator and photosensor, accurate energy measurement was not required, and the circuit was designed to enforce only a simple energy window. This Application Specific Integrated Circuit (ASIC) is 3.3 mm × 4.5 mm in size and consumes only 117 mW of power, minimizing undesirable heating. Twelve of these modular detectors (LYSO + APD + ASIC) form the complete PET ring (Fig. 1b) and require only a single flexible cable for all power, data and programming functions.

We built a data acquisition module that digitizes the time of the gamma interaction to the subnanosecond level and serializes the

data for transmission through a single optical fiber to the host PC¹⁸. We recorded all single events to disk and developed offline software to select prompt and delayed coincidences¹⁹, bin them into fully three-dimensional sinograms and reconstruct quantitative PET images (Online Methods). We demonstrated quantitative performance of this set-up in a multicompartiment phantom study that compared radioactivity concentrations measured by the RatCAP with those measured using aliquots in a calibrated well counter (Fig. 1c). Preliminary data from a rat brain showed good overall quality, correspondence with a rat atlas and sufficient sensitivity for neurotransmitter studies such as [^{11}C]raclopride scans of the dopamine D₂ receptor system (Fig. 1d).

Animal mobility system

As the weight of the scanner is a substantial fraction of the rat's weight, we devised a mechanical system to facilitate rat movement. We suspended the scanner on long springs with low spring rate so the rat could move the scanner up and down several centimeters and across the floor of the experimental chamber with only a small change in spring force (Fig. 2a). To stabilize the motion and allow routing of cables, we fastened the springs to a lightweight telescoping structure with linear bearings for vertical motion. We attached this structure at the top to a fixed frame by a gimbaled pivot to allow pendulum-like motion across the full chamber (Fig. 2b). We used needle bearings to allow the structure to rotate about its axis. The resulting mechanism allowed essentially frictionless motion with almost full freedom in the 40 × 40 cm Plexiglas chamber (Fig. 2c,d). To illustrate the motion of rats wearing the RatCAP, we present drawings of rat trajectories in the test chamber (Fig. 2d). Movement is restricted mainly by the inertia of the device, although we are exploring an active motorized tracking system to mitigate this constraint.

Although the scanner moves freely, it must be rigidly fastened to the rat to prevent motion artifacts in the PET image. We surgically secured an attachment bracket to the outside of the skull for this purpose (Fig. 2e,f). For most of the data presented here, the bracket was a short section of aluminum tube that had to be attached to the rat with screws before the scan (Fig. 2e). In the latest version of the system, the bracket is small and can be worn permanently (Fig. 2f). After the rat's head is guided into the scanner, a magnetic tip on the bracket automatically latches onto

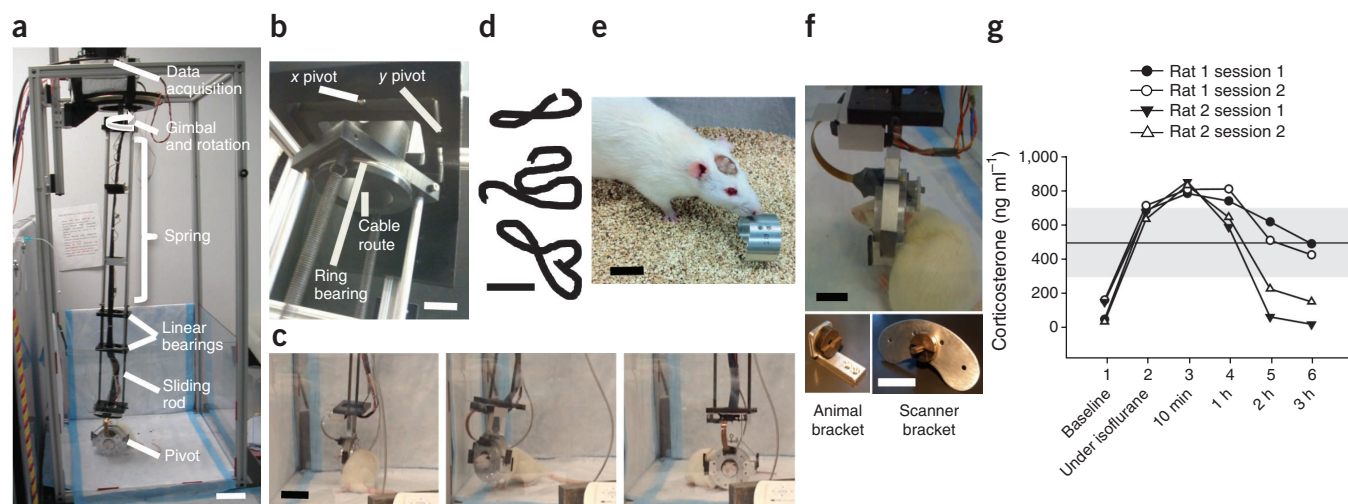


Figure 2 | Animal mobility system. **(a)** Overview of key components of the animal mobility system. Scale bar, 8 cm. **(b)** Detail of top gimbal and rotation mechanism. Scale bar, 2 cm. **(c)** Three video frames exemplifying the typical range of motion of a rat wearing the PET scanner inside the chamber. Scale bar, 4 cm. **(d)** Drawings of actual trajectories made by the rat in the $40 \times 40 \text{ cm}^2$ test chamber. Tracks reflect the position of the rat's approximate center. Scale bar, 15 cm. **(e)** Photograph of a rat showing the result of surgery performed to affix screw sockets and a sleeve to attach the PET scanner to its head. Scale bar, 2 cm. **(f)** Photographs showing the improved, self-latching mounting mechanism that obviates the need for momentary anesthesia during attachment, including latched brackets (top), a detail of an animal bracket (bottom left) and a detail of a scanner bracket (bottom right). Scale bars, 2 cm. **(g)** Corticosterone levels in rat blood plasma measured at different time points of wearing the RatCAP. The measurements were performed on two occasions (sessions 1 and 2) that were 14 d apart. Sampling took place before and 10 min, 1 h, 2 h and 3 h after attachment of the RatCAP. The horizontal line (mean) and shaded area (\pm s.d.) indicate the levels of corticosterone in a group of rats ($n = 10$) that underwent only transport between rooms 30 min before the blood sampling.

a mating piece on the scanner. The earlier procedure required momentary anesthesia with isoflurane, and the new method was devised to eliminate this step.

Although the rats appeared to adapt well to the device and move freely about the enclosure, we assessed the degree of stress quantitatively by measuring corticosterone in blood as a function of time wearing the scanner. Although corticosterone concentrations increased initially (owing to isoflurane anesthesia and exposure to the RatCAP), they decreased over time while the tomograph was attached (Fig. 2g). This decrease occurred to different degrees between the rats, in one case reflecting a return to baseline levels common to rats left undisturbed in the home cage and in the other reaching levels similar to those observed in rats that we transported in their home cages a short distance between rooms 30 min before the sample was taken (Fig. 2g). Transport usually precedes animal experimentation and is not typically considered an intervention, although it is accompanied by wakefulness and exploratory activity and may be stressful. Rats wearing the RatCAP did not show habituation (a decrease

in corticosterone) over test sessions, possibly owing to the long interval (14 d) between the test sessions.

Behavioral neuroimaging

First, we compared the [^{11}C]raclopride PET scans of five female rats that we imaged while awake and then again 1 h later under ketamine-xylazine anesthesia. Although anesthesia represented an experimental treatment, it is a prerequisite for typical small-animal PET studies. Thus, data from the anesthetized state also represented a standard against which we could compare data from the awake, behaving condition. Moreover, we could use the PET data from the awake condition for correlation with behavioral data. Initially, we used the most common approach to PET radiotracer administration, a bolus injection in which the entire dose was given in less than 1 min. Averaged time activity curves for the two conditions had the expected shape, with radiotracer uptake peaking shortly after the injection and leveling off over the remaining time of the scan (Fig. 3a). The overall uptake of [^{11}C]raclopride (averaged over the last 30 min of the scans) was

Figure 3 | D2 receptor neuroimaging using bolus injections of [^{11}C]raclopride in the behaving and anesthetized rat. **(a)** Activity concentrations of the radiotracer (nCi ml^{-1}) over time in different brain regions. Concentrations are normalized to the injected tracer dose (0.19–0.97 mCi of [^{11}C]raclopride with a raclopride mass of $1.5\text{--}7.9 \text{ nmol kg}^{-1}$). The data show average concentrations for the awake scans and scans performed under anesthesia (mean \pm s.e.m., $n = 5$). Comparisons reflect t tests for paired samples. $**P < 0.01$. **(b)** Estimate of specific binding of [^{11}C]raclopride in the striatum. STR, striatum uptake; CB, cerebellum uptake. Bars indicate BP_{ND} (mean \pm s.e.m., $n = 5$) for the awake and anesthetized (anes.) states (paired t test, $P = 0.18$). **(c)** Behavioral activity summed for the last 30 min of the awake scans and plotted against specific binding in the striatum for [^{11}C]raclopride ($(\text{STR} / \text{CB}) - 1$) (Spearman $r = 0.9$, $P = 0.04$, $n = 5$). All scores indicate ranks. A rank of 1 reflects the lowest score.

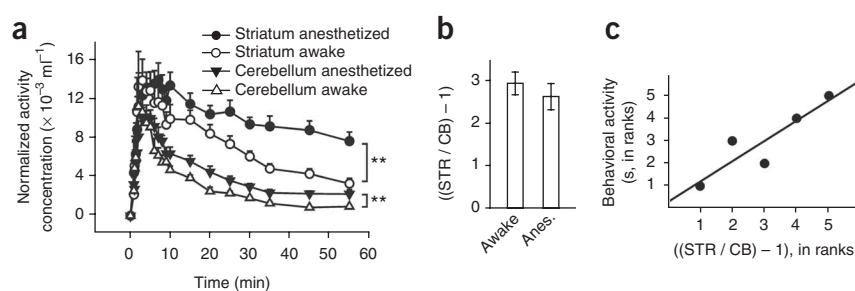
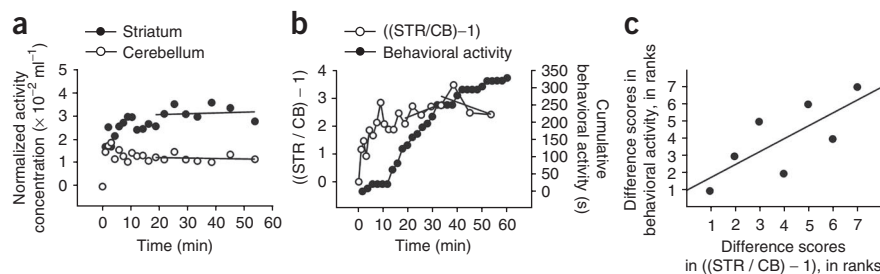


Figure 4 | Transient changes in BP_{ND} in relation to behavioral activity during the PET scan. **(a)** Activity concentrations of the radiotracer [^{11}C]raclopride ($nCi\ ml^{-1}$) over time in different brain regions of an individual rat, normalized to the total injected dose (0.28 mCi of [^{11}C]raclopride with a raclopride mass of 2.0 $nmol\ kg^{-1}$), using B-I infusion. The relative flatness of the regression line fitting the cerebellum data indicates a steady-state condition of the radiotracer. **(b)** Estimate of specific binding in the striatum for [^{11}C]raclopride $((STR/CB) - 1)$ and cumulative behavioral activity measured simultaneously in the same rat. Each point on the behavioral response curve reflects the summed activity over a 2-min period. A slope in the response curve indicates that the rat showed activity, whereas flat regions indicate the absence of activity. Regression lines show the changes in the slope of the behavioral response curve which reflect the slope changes in $((STR/CB) - 1)$. **(c)** Correlation of PET and behavioral data for data points starting at 20 min in **b**. We subtracted every two successive time points on the PET curve $((STR/CB) - 1)$ and used the difference scores for correlation with the behavioral data. We cumulated behavioral activity for the time frames provided by the PET data and used the differences between successive time points for correlation analysis. Spearman $r = 0.75$; $P = 0.05$. All scores indicate ranks. A rank of 1 reflects the lowest score.



significantly higher in anesthetized than in awake, behaving rats, in both the striatum (paired t test, $P = 0.005$) and cerebellum (paired t test, $P = 0.003$). We measured an estimate of the binding potential (BP), which is the ratio of tracer concentration in receptor-rich over receptor-free brain tissue ($BP_{ND} = (\text{striatum} / \text{cerebellum}) - 1$), where ND reflects free and nondisplaceable (ND) uptake of the tracer²⁰ (Online Methods). Variations in binding potential depend on the amount of endogenous ligand that is bound to the receptors²¹. For example, a higher level of receptor occupancy by endogenous dopamine translates into a lower binding potential of [^{11}C]raclopride, because fewer binding sites are available for occupancy by the radiotracer. Anesthesia resulted in a 10.6% reduction in BP_{ND} , indicative of a reduction in D_2 receptor availability in the striatum (Fig. 3b), although the difference did not reach significance. Studies in humans and other animals (conscious, restrained primates or cats) have examined the effects of ketamine on the binding potential of [^{11}C]raclopride, with mixed results. Although some studies reported a significant decrease in striatal binding potential, others did not²². To our knowledge, ours is the only study that found an increase in cerebellar uptake under ketamine anesthesia. Changes in cerebral

blood flow, nonspecific binding or peripheral clearance of the radiotracer could have contributed to these results^{21,23}, as well as the fact that the rats were not only awake but also behaviorally active during the scan.

The data from the awake, behaving condition showed that the extent of behavioral activity (the summed duration of head turns, forward movement and movement of the body without movement of the head; see Online Methods for full definition) was positively correlated with BP_{ND} in the striatum (Fig. 3c). The correlation indicates that lower D_2 receptor occupancy by dopamine coincided with higher behavioral activity or, conversely, that higher dopamine D_2 receptor binding predicted lower behavioral activation. This is perhaps a counterintuitive result, because behavioral activation is typically associated with an increase in dopamine release. However, the direction of the results would also depend on the site of action of dopamine. For example, D_2 autoreceptor activation by low doses of the D_2 agonist quinpirole inhibits behavioral activity^{24,25}. Thus it is possible that the PET data are sensitive to variations in D_2 autoreceptor occupancy. Overall, our new method provides data that may challenge current models and ultimately improve our understanding of the dopamine system.

A limitation of the bolus injection method we used above is its insensitivity to the transient changes in BP_{ND} that occur during the PET scan, which may relate to changes in type and degree of behavioral expression. The bolus and infusion (B-I) method establishes a constant level of radiotracer in tissues and allows the detection of perturbations from equilibrium resulting from interventions during the scan²⁶. Thus, the B-I method seems to be ideal for studying transient changes in BP_{ND} that may correlate with behavior. To examine this possibility, we first established the

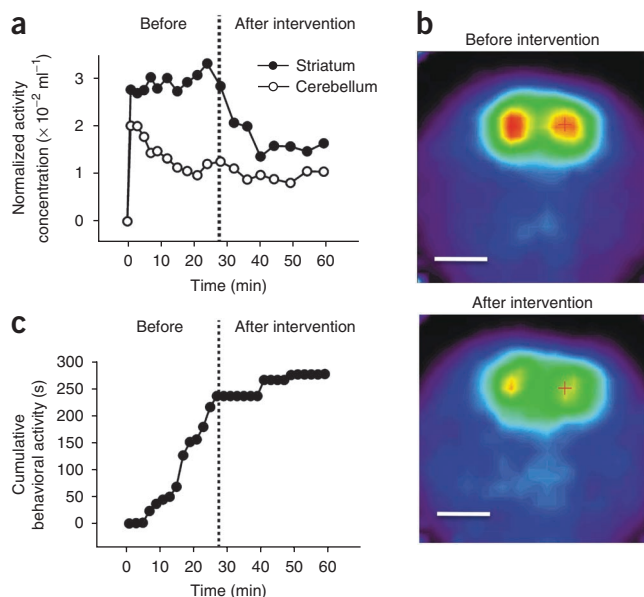


Figure 5 | Transient changes in BP_{ND} and behavior after D_2 receptor blockade. **(a)** Activity concentrations of the radiotracer [^{11}C]raclopride ($nCi\ ml^{-1}$) over time in different brain regions of an individual rat, normalized to the total injected dose (0.4 mCi of [^{11}C]raclopride with a raclopride mass of 2.5 $nmol\ kg^{-1}$), using B-I infusion. Dashed line indicates infusion of cold raclopride (2 $mg\ kg^{-1}$; intravenously (i.v.), in less than 1 min). **(b)** Images showing uptake of [^{11}C]raclopride before and after the intervention with cold raclopride. Scale bars, 6 mm. **(c)** Cumulative behavioral activity before and after the intervention with cold raclopride. Each dot reflects the summed activity over 2 min. A slope in the response curve indicates that the rat showed activity, whereas flat regions indicate the absence of activity.

infusion parameters necessary to maintain a steady-state condition of [^{11}C]raclopride in awake, behaving rats. We found that equilibrium in the striatum was achieved when 40% of the total injected dose was infused as a bolus, followed by the remaining 60% at a constant low infusion rate over the remainder of the 1-h scan (Fig. 4a). Notably, these parameters are different from those needed to establish equilibrium in the anesthetized state, which were 60% and 40%, respectively. We then investigated whether we could directly relate the changes in behavioral activity to changes in BP_{ND} of [^{11}C]raclopride in the striatum. We found that periods of behavioral activity coincided with a slope increase in BP_{ND} and periods of inactivity with a slope decrease in BP_{ND} (Fig. 4b), consistent with the correlation we reported above (Fig. 3c). When we correlated changes between the data points on the PET curve (Fig. 4b) with changes in behavioral activity (which we cumulated for the time frames provided by the PET data), we also found a positive correlation between the PET and behavioral data (Fig. 4c). An increase in BP_{ND} coincided with an increase in behavioral activity, and, conversely, a decrease in BP_{ND} was accompanied by a decrease in behavioral activation.

We then investigated whether we could assess drug effects simultaneously on BP_{ND} and behavior by the same B-I method. We intervened 27.5 min into the scan with a physiologically active dose of unlabeled raclopride. This reduced the uptake of [^{11}C]raclopride in the striatum by more than 50%, with peak effects achieved after ~10 min, and continued to block the uptake of [^{11}C]raclopride for the remainder of the scan (Fig. 5a). The corresponding images before and after the intervention reflect the changes in uptake in the striatum (Fig. 5b). We analyzed behavioral activity for the same rat. The pharmacological dose of the D_2 antagonist raclopride had an inhibiting effect on behavior (Fig. 5c), consistent with previously published studies^{27,28}. Thus, our method may be used for the direct correlation of PET and behavioral data under natural conditions as well as in drug studies.

DISCUSSION

The RatCAP scanner is a fully functional PET system with spatial resolution comparable to commercially available small-animal PET systems²⁹. Although its coincidence sensitivity is limited by physical constraints, our data indicate that it is sufficient for [^{11}C]raclopride studies of the dopamine system. The passive mechanical attachment system allows for a considerable range of behavior across space. In the future, active electromechanical designs may provide even more flexibility. Our data also suggest that the B-I method of radiotracer administration can be used to study the relationship between radiotracer binding and behavior.

A legitimate question is how the temporal resolution of PET can account for correlations with behavior. The ability of PET to measure function over time is a complex issue that has not been fully explored. In typical bolus neuroreceptor studies, the temporal resolution might be thought of as the time between scans (for example, hours), because although the PET data may be collected dynamically each scan ultimately produces a single functional measure with respect to time. With B-I administration, one could argue that it is the time required to reestablish tracer equilibrium after a change in receptor occupancy, because equilibrium is a prerequisite for absolute quantification of receptor availability. This can be several minutes (Fig. 5), although it will depend on

the kinetics of the particular tracer used. However, as we show here, tracer binding begins to change on a much shorter time scale, which implies that it may reflect relative changes in receptor occupancy in a fast if not fully quantitative manner. We speculate that this effect underlies our observed correlation between changes in behavior and changes in receptor binding. In contrast, the fact that equilibration occurs over a longer time scale suggests that our correlations might be improved by introducing a time delay between the two data sets, an idea that we will explore in future work.

In conclusion, our studies suggest that in rats PET and behavioral data can be simultaneously acquired and that correlations between the data sets are possible. A future application of this method will be the study of sexual behavior in relation to dopamine receptor binding. Given the wide range of PET radiotracers and behavioral measures available to probe various aspects of brain function, this multidimensional approach can have considerable potential for yielding new insights into brain function.

METHODS

Methods and any associated references are available in the online version of the paper at <http://www.nature.com/naturemethods/>.

Note: Supplementary information is available on the Nature Methods website.

ACKNOWLEDGMENTS

We thank W. Lenz for mechanical design and fabrication; D. Alexoff for assistance with rat handling; S. Park for coincidence-processing methods; W. Schiffer for assistance with data analysis; C. Reiszal for expertise in catheter design; V. Radeka, R. Lecomte and R. Fontaine for contributions to the electronics; J. Logan for advice on kinetic modeling; J. Fowler and the personnel of the Brookhaven National Laboratory PET center and cyclotron for making the radiotracers available for our studies and N. Volkow for proposing the idea of a conscious-animal PET scanner. The research was carried out at Brookhaven National Laboratory under contract number DE-AC02-98CH10886 with the US Department of Energy and funded by the Department of Energy's Office of Biological and Environmental Research.

AUTHOR CONTRIBUTIONS

D.S. proposed and carried out most of the rat work, acquired and analyzed behavioral data and wrote the paper. S.S. developed quantitative PET data processing and reconstruction software and acquired and analyzed PET data. S.S.J. developed front-end and data acquisition electronics, software and firmware. J.-F.P. developed the front-end microchip. M.L.P. developed data processing and image reconstruction software. S.P.S. assembled and debugged scanner and mechanics. B.R. and S.H.M. acquired rat data and performed data analysis. S.K. constructed scanner components. F.A.H. contributed to the behavioral neuroimaging experiments. P.O. oversaw and conceived key aspects of the electronics. C.L.W. oversaw development of the scanner, especially the front-end detectors and electronics. D.J.S. oversaw development of the scanner and performed rat studies and data analysis. P.V. oversaw development of the scanner, software and mechanics, performed rat studies and wrote the paper.

COMPETING FINANCIAL INTERESTS

The authors declare no competing financial interests.

Published online at <http://www.nature.com/naturemethods/>.

Reprints and permissions information is available online at <http://npg.nature.com/reprintsandpermissions/>.

- Schultz, W. Multiple dopamine functions at different time courses. *Annu. Rev. Neurosci.* **30**, 259–288 (2007).
- Clark, J.J. *et al.* Chronic microsensors for longitudinal, subsecond dopamine detection in behaving animals. *Nat. Methods* **7**, 126–129 (2010).
- Westerink, B.H.C. Brain microdialysis and its application for the study of animal behaviour. *Behav. Brain Res.* **70**, 103–124 (1995).

4. Dombeck, D.A., Khabbazi, A.N., Collman, F., Adelman, T.L. & Tank, D.W. Imaging large-scale neural activity with cellular resolution in awake, mobile mice. *Neuron* **56**, 43–57 (2007).
5. Momosaki, S. *et al.* Rat-PET study without anesthesia: anesthetics modify the dopamine D1 receptor binding in rat brain. *Synapse* **54**, 207–213 (2004).
6. Patel, V.D., Lee, D.E., Alexoff, D.L., Dewey, S.L. & Schiffer, W.K. Imaging dopamine release with positron emission tomography (PET) and ¹¹C-raclopride in freely moving animals. *Neuroimage* **41**, 1051–1066 (2008).
7. Hosoi, R. *et al.* MicroPET detection of enhanced ¹⁸F-FDG utilization by PKA inhibitor in awake rat brain. *Brain Res.* **1039**, 199–202 (2005).
8. Harada, N., Ohba, H., Fukumoto, D., Kakiuchi, T. & Tsukada, H. Potential of [¹⁸F]β-CFT-FE (2β-carbomethoxy-3β-(4-fluorophenyl)-8-(2-[¹⁸F]fluoroethyl) nortropane) as a dopamine transporter ligand: a PET study in the conscious monkey brain. *Synapse* **54**, 37–45 (2004).
9. Itoh, T. *et al.* PET measurement of the *in vivo* affinity of ¹¹C-(R)-rolipram and the density of its target, phosphodiesterase-4, in the brains of conscious and anesthetized rats. *J. Nucl. Med.* **50**, 749–756 (2009).
10. Ferris, C.F. *et al.* Functional magnetic resonance imaging in conscious animals: a new tool in behavioural neuroscience research. *J. Neuroendocrinol.* **18**, 307–318 (2006).
11. Kyme, A.Z., Zhou, V.W., Meikle, S.R. & Fulton, R.R. Real-time 3D motion tracking for small animal brain PET. *Phys. Med. Biol.* **53**, 2651–2666 (2008).
12. Grace, A.A. The tonic/phasic model of dopamine system regulation: its relevance for understanding how stimulant abuse can alter basal ganglia function. *Drug Alcohol Depend.* **37**, 111–129 (1995).
13. Kravitz, A.V. *et al.* Regulation of parkinsonian motor behaviours by optogenetic control of basal ganglia circuitry. *Nature* **466**, 622–626 (2010).
14. White, N.M. Addictive drugs as reinforcers: multiple partial actions on memory systems. *Addiction* **91**, 921–949 (1996).
15. Wise, R.A. Dopamine, learning and motivation. *Nat. Rev. Neurosci.* **5**, 483–494 (2004).
16. Vaska, P. *et al.* RatCAP: miniaturized head-mounted PET for conscious rodent brain imaging. *IEEE Trans. Nucl. Sci.* **51**, 2718–2722 (2004).
17. Pratte, J.-F. The RatCAP front-end ASIC. *IEEE Trans. Nucl. Sci.* **55**, 2727–2735 (2008).
18. Junnarkar, S.S. *et al.* Next generation of real time data acquisition, calibration and control system for the RatCAP scanner. *IEEE Trans. Nucl. Sci.* **55**, 220–224 (2008).
19. Park, S.J. *et al.* Digital coincidence processing for the RatCAP conscious rat brain PET scanner. *IEEE Trans. Nucl. Sci.* **55**, 510–515 (2008).
20. Innis, R.B. *et al.* Consensus nomenclature for *in vivo* imaging of reversibly binding radioligands. *J. Cereb. Blood Flow Metab.* **27**, 1533–1539 (2007).
21. Laruelle, M. Imaging synaptic neurotransmission with *in vivo* binding competition techniques: a critical review. *J. Cereb. Blood Flow Metab.* **20**, 423–451 (2000).
22. Rabiner, E.A. Imaging of striatal dopamine release elicited with NMDA antagonists: is there anything to be seen? *J. Psychopharmacol.* **21**, 253–258 (2007).
23. Hassoun, W. *et al.* PET study of the [¹¹C]raclopride binding in the striatum of the awake cat: effects of anaesthetics and role of cerebral blood flow. *Eur. J. Nucl. Med.* **30**, 141–148 (2003).
24. Eilam, D. & Szechtman, H. Biphasic effect of D-2 agonist quinpirole on locomotion and movements. *Eur. J. Pharmacol.* **161**, 151–157 (1989).
25. Li, S.-M. Yawning and locomotor behavior induced by dopamine receptor agonists in mice and rats. *Behav. Pharmacol.* **21**, 171–181 (2010).
26. Carson, R.E. PET physiological measurements using constant infusion. *Nucl. Med. Biol.* **27**, 657–660 (2000).
27. Hillegaart, V. & Ahlenius, S. Effects of raclopride on exploratory locomotor activity, treadmill locomotion, conditioned avoidance behaviour and catalepsy in rats: behavioural profile comparisons between raclopride, haloperidol and preclamol. *Pharmacol. Toxicol.* **60**, 350–354 (1987).
28. van den Boss, R., Cools, A.R. & Ogren, S.-O. Differential effects of the selective D2-antagonist raclopride in the nucleus accumbens of the rat on spontaneous and *d*-amphetamine-induced activity. *Psychopharmacology (Berl.)* **95**, 447–451 (1988).
29. Larobina, M., Brunetti, A. & Salvatore, M. Small animal PET: a review of commercially available imaging systems. *Curr. Med. Imaging Rev.* **2**, 187–192 (2006).
30. Paxinos, G. & Watson, C. *The Rat Brain in Stereotaxic Coordinates* 6th edn., 243 (Elsevier, London, 2007).

ONLINE METHODS

RatCAP performance measurement. For the measurement of spatial resolution, a ^{68}Ge point source was imaged at multiple locations across the field of view (~2 mm increments, from center to edge). Each data set was reconstructed with the methods used for rat imaging described below, except without Gaussian filtering. Radial and tangential line profiles were drawn through the image of each point and the respective FWHM determined. Coincidence sensitivity was measured with a ^{22}Na point source centered in the field of view. It is reported as a ratio of true coincidence event rate measured with the RatCAP to the decay rate by positron branch as measured in a calibrated ion chamber.

Rats. Female adult Sprague Dawley rats (250–300 g) of a strain selectively bred at Brookhaven National Laboratory (congenital nonlearned helpless (cNLH)^{31,32}) were used in the experiments. They were housed in pairs until surgery and individually thereafter in standard polycarbonate cages. The rats were maintained on a 12-h:12-h light:dark cycle (lights on at 7:00 a.m.) with free access to food and water. All procedures were approved by the Brookhaven National Laboratory Institutional Animal Care and Use Committee and were conducted in accordance with the US National Institutes of Health *Guide for the Care and Use of Laboratory Animals*.

Surgeries. Jugular vein catheters were implanted for radiotracer infusion, drug administration and blood sampling. Head surgeries were performed for later attachment of the RatCAP scanner. The surgeries were done within the same session 4–5 d before the experiments. The jugular vein catheters consisted of 10 cm of silastic tubing with an inner diameter of 0.30 mm (HelixMark). One end was fitted over a stainless steel tube (1 cm long) that projected to the side of a back-mount cannula connector pedestal (Plastics One). Short strips of silastic tubing additionally sheathed and protected the catheter tubing around the steel tube. The loose end of the catheter tubing was inserted ~2 cm into the jugular vein and secured with sutures. A silicone bead on the tubing served as an anchor for the sutures. The connector pedestal, which had polyester mesh on the base, was mounted subcutaneously on the back of the rat. To ensure catheter patency, the lines were flushed every 3 d with 200 $\mu\text{g ml}^{-1}$ gentamicin solution (Sigma-Aldrich). Screw sockets were mounted on the exterior of the skull to accept a tubular sleeve that slides into the RatCAP scanner. The rat was positioned in a stereotaxic apparatus (David Kopf Instruments), and the skull was cleaned with 30% (wt) hydrogen peroxide in water (Sigma-Aldrich) until completely dry. Up to eight holes were drilled into the skull away from the midline to suit anchor screws for stability of the dental cap. A 2-octyl-cyanoacrylate-based tissue adhesive (Meridian Animal Health) was applied to the skull to affix two screw sockets (7 mm high, 3 mm wide). They were placed at a distance of 7 mm from each other, spanning approximately the midline from bregma to lambda. Dental cement (Lang Dental) was immediately applied to the skull. Layers of cement were added to seal the sockets except for their openings on the top.

Attachment of RatCAP and infusion lines. Imaging data were acquired before implementation of the self-latching magnetic bracket to secure the rat. To facilitate mounting the scanner,

the rat was anesthetized with a bolus of short-acting isoflurane gas. The tubular sleeve was attached to the head sockets with screws, aligned with the RatCAP and locked. An infusion line was attached to the cannula pedestal on the back of the rat. The infusion lines consisted of 120-cm-long PE50 tubing. A Y-connector allowed for simultaneous infusions of the radiotracer and drugs. Standard glass microsyringes (5 ml) were used to deliver the fluids. Infusion rates and volumes were controlled by a syringe pump (CMA Microdialysis). A step-by-step protocol describing the attachment of the RatCAP and infusion lines is available in the **Supplementary Note**.

Open field. The rat was given ~1 h to acclimate to the RatCAP before the experiments. Throughout this time and during the experiments, the rat was kept in a square open field (40 × 40 × 40 cm³) made of transparent Plexiglas. The flooring and two of the sides were cushioned with absorbent towels. A video camera (Sony, DCR-SR40) was placed ~1.5 m away from the open field. All experiments were filmed sideways, and the behavior was analyzed afterward.

Radiochemistry. [^{11}C]raclopride was synthesized and formulated for injection by a method adapted from a previously published study³³. Briefly, 4 μl of 5 N NaOH was added to 1.5 mg of nor-raclopride in 0.2 ml of DMSO (Sigma-Aldrich), and the mixture was vortexed for ~2 min until the solution turned dark green. The solution was stored under argon until [^{11}C]methyl iodide synthesis was complete. The [^{11}C]methyl iodide was released from an automated synthesis unit in a stream of argon that was passed through the solution slowly at 20 °C. When the [^{11}C]methyl iodide transfer was complete, the reaction was heated at 80 °C for 2 min. At the end of heating, 0.2 ml of 0.3 M HCl was added to the reaction vessel followed by 0.8 ml of water. The mixed contents were then loaded into an injection loop for purification by reversed-phase HPLC (Phenomenex Gemini C18 (250 mm × 10 mm, 5 μm)) eluting with MeOH–ammonium formate (0.1 N) in a 1:1 ratio. The precursor elutes with a retention time of ~12.5 min, and the final product, [^{11}C]raclopride, elutes at ~17.2 min. The product was collected and concentrated by rotary evaporation and azeotroping with 1–2 ml of acetonitrile. The residue was blown to final dryness with a stream of nitrogen to ensure the removal of residual organic solvent. The dried product was then dissolved in 5 ml of saline (USP) and filtered through a sterile filter into a sterile multi-injection vial. A sample was retained for quality control that included thin-layer chromatography and pyrogen and sterility testing. The chemical and radiochemical purity and specific activity was determined by thin-layer chromatography and by HPLC. Specific activities (at the time of injection) for [^{11}C]raclopride were maintained at 0.5 Ci μmol^{-1} or greater.

Radiotracer infusion protocols. For bolus infusions, injected doses of [^{11}C]raclopride were ~1 mCi (i.v.) or less with total raclopride mass maintained at tracer levels; the average mass was 5.16 (± 2.39 s.d.) nmol kg^{-1} for the awake scans and 4.69 (± 1.95 s.d.) for the scans under anesthesia. Approximately 30–45 min before the second scan, an initial dose of ~6 mg per kg body weight (i.v.) ketamine (and xylazine, in a ratio of 10:1) was given followed by maintenance doses of 20–40 mg per kg body weight (intraperitoneally) every 30 min or as needed to achieve respiration rates of 48–60

breaths min^{-1} (see **Supplementary Note** for a detailed protocol on radiotracer infusions in the awake and anesthetized rat). For B-I, 40% of the total injected dose was infused as a bolus in less than 1 min and followed by the remaining 60% at a constant low rate (rate = 60% of total dose per hour).

Blood sampling and analysis. Blood samples (up to 0.5 ml) were collected from the jugular vein via indwelling catheters that were also used for radiotracer infusion in our PET studies. Sampling took place on two occasions, separated by 2 weeks, between ~12:00 p.m. and ~4:00 p.m. to simulate the time schedule of our imaging experiments. The first sample (baseline) was taken immediately from the home cage, which was left undisturbed for at least 24 h before the sample was taken. The rat was then anesthetized with a bolus of isoflurane and the sleeve attached. The second sample was taken during anesthesia shortly before the rat was locked in the RatCAP. A third sample was taken 10 min after waking. Every other hour, the fourth, fifth and sixth samples were collected. In a separate experiment, blood samples were collected from the dorsal tail vein 30 min after transport between rooms. All samples were kept on ice until centrifuged at $17.9 \times 10^3 \text{g}$ (13,000 r.p.m. in an Eppendorf rotor FA-45-30-11) and 4°C for 15 min. The plasma was collected and stored at -20°C until analyzed for corticosterone according to the manufacturer's protocol (^{125}I RIA kit; MP Biomedicals).

Data analysis. The imaging data were processed offline to produce prompt and delayed-coincidence (randoms) sinograms with 47 radial and 24 azimuthal bins. The coincidence window (2τ) was 18 ns, and the energy threshold was 350 keV. Sinograms were reconstructed with the maximum likelihood expectation maximization algorithm, for which the system matrix was generated by separately simulating sources of radioactivity within each voxel on a ~1-mm grid using a Monte Carlo simulation of the PET system. The reconstruction included corrections for attenuation, scatter (simulated in the system matrix assuming uniform tissue distribution through the field of view) and random coincidences (added after the forward projection step) (S.S., M.L.P., D.J.S., C.L.W. & P.V.; unpublished data). Each time frame was reconstructed using 100 iterations and post-smoothing with a 1.8-mm FWHM Gaussian kernel. Regions of interest (ROIs) were drawn on the relevant brain areas with ASIPro software (Siemens). Each striatum ROI was 75 mm^3 , and the cerebellum ROI was

250 mm^3 . Decay-corrected time-activity curves were generated and averaged for the left and right sides of the brain. The cerebellum is devoid of D_2 receptors³⁴ and was used as a reference region representing free and nonspecific or nondisplaceable uptake²⁰. The striatum-to-cerebellum ratio ($\text{BP}_{\text{ND}} = (\text{STR} - \text{CB}) / \text{CB} = (\text{STR} / \text{CB}) - 1$) at equilibrium was taken to indicate specific binding of the radiotracer. BP_{ND} was calculated as the average of the ratio over the last five data points on the time-activity curve spanning the last 30 min of the scans unless otherwise indicated. The difference between the awake and anesthetized conditions was assessed with the equation $\Delta\text{BP}_{\text{ND}} = (1 - \text{BP}_{\text{ND}} \text{ anes} / \text{BP}_{\text{ND}} \text{ awake}) \times 100\%$. Behavioral activity was measured from videotape using the manual function of EthoVision software (Noldus) and included all forms of movement, that is, head turns, forward movement, movement of the body without movement of the head, but not the repositioning of the legs while sitting, chewing and movements related to breathing and sniffing that were not accompanied by locomotion. Rearings, a vertical form of exploration, and grooming behavior were not observed in rats wearing the RatCAP and therefore did not contribute to the definition of behavioral activity. The software files necessary to process data from the RatCAP scanner into images, including coincidence processing and image reconstruction, are available as **Supplementary Software**.

Statistical analyses. All data used for statistical evaluations were checked for normality of the distributions by the Shapiro-Wilks test. Nonparametric statistics were used when the assumption of normality was violated. The Spearman rank-order correlation was used to assess the relationships between two variables. When parametric statistics were applied, the *t* test for paired samples was used for comparison of repeated measures. $P \leq 0.05$ (two-tailed) were considered significant.

31. Henn, F.A. & Vollmayr, B. Stress models of depression: Forming genetically vulnerable strains. *Neurosci. Biobehav. Rev.* **29**, 799–804 (2005).
32. Schulz, D., Mirrione, M.M. & Henn, F.A. Cognitive aspects of congenital learned helplessness and its reversal by the monoamine oxidase (MAO)-B inhibitor deprenyl. *Neurobiol. Learn. Mem.* **93**, 291–301 (2010).
33. Ehrin, E. *et al.* Preparation of ^{11}C -labelled raclopride, a new potent dopamine receptor antagonist: Preliminary PET studies of cerebral dopamine receptors in the monkey. *Int. J. Appl. Radiat. Isot.* **36**, 269–273 (1985).
34. Sesack, S.R., Aoki, C. & Pickel, V.M. Ultrastructural localization of D_2 receptor-like immunoreactivity in midbrain dopamine neurons and their striatal targets. *J. Neurosci.* **14**, 88–106 (1994).